JOURNAL OF VIROLOGY, July 1995, p. 4069–4078 Vol. 69, No. 7
0022-538X/95/$04.00+0

The Murine AIDS Defective Provirus Acts as an Insertional Mutagen in Its Infected Target B Cells

MING HUANG,[1] MIRKO TAKAC,[1]† CHRISTINE A. KOZAK,[2] AND PAUL JOLICOEUR[1,3,4]*

Laboratory of Molecular Biology, Clinical Research Institute of Montreal, Montréal, Québec, Canada H2W 1R7[1]; Département de Microbiologie et d'Immunologie, Université de Montréal, Montréal, Québec, Canada H3J 3J7[3]; National Institute of Allergy and Infectious Diseases, Bethesda, Maryland 20892[2]; and Department of Experimental Medicine, McGill University, Montréal, Québec, Canada H3G-1A4[4]

Received 14 December 1994/Accepted 3 April 1995

In susceptible mice, the murine AIDS (MAIDS) defective virus can induce marked expansion of its target cells, the majority of which belong to the B-cell lineage. This expansion, which appears to be critical for the development of the immunodeficiency syndrome, is initially polyclonal but becomes oligoclonal late in the disease, suggesting the involvement of a secondary genetic event(s) during this proliferation. To determine whether integration of the MAIDS defective provirus into particular regions of the cellular genome contributes to this oligoclonal expansion, we searched for common provirus integration sites in enlarged lymphoid organs of MAIDS mice. We identified two common proviral integration sites, Dis-1 and Dis-2, which were occupied by a defective provirus at frequencies of 20 and 13%, respectively. Our analysis revealed that the Dis-1 region corresponds to the *Sfpi1* (Spi-1, PU.1) locus, which maps on chromosome 2, and encodes a transcription factor. Insertion of the MAIDS defective provirus into this region led to a two- to threefold increase in the expression of *Sfpi1* RNA. The Dis-2 locus was found to map to mouse chromosome 11, between *Hox2* and *Scya*. It appears to be a novel locus probably harboring a gene involved in B-cell proliferation. The present study indicates that the MAIDS defective provirus can act as an insertional mutagen, thus contributing to the oligoclonal expansion of infected cells. The detection of two common proviral integration sites, each of which targetted at a low frequency in diseased organs, suggests that the deregulation of a unique gene through provirus insertion is essential for neither proliferation of infected B cells nor development of the immunodeficiency syndrome.

Murine AIDS (MAIDS) is characterized by splenomegaly, lymphadenopathy, hypergammaglobulinemia, and T- and B-cell dysfunctions (for reviews, see references 30, 43, and 44). The disease is induced by a defective murine leukemia virus (MuLV) (2, 10). Although the MAIDS defective virus requires a helper MuLV for replication (2, 11), we previously found that induction of the immunodeficiency syndrome is not dependent on viral replication, as helper-free stocks of the MAIDS defective virus could induce disease when inoculated into susceptible C57BL/6 mice (27). We found that in the absence of replicating helper viruses, the MAIDS defective virus could induce marked expansion of its target cells (27, 29). The majority of these proliferating cells infected by the defective virus were found to belong to the B-cell lineage (29). Proliferation of these infected B cells appears to be essential for development of the disease, since a close correlation between their proliferation and the susceptibility of several mouse strains to the immunodeficiency syndrome has been observed (28). However, it is still not clear how infection of these B cells eventually leads to severe dysfunctions of lymphoid T cells. Moreover, the mechanisms by which the MAIDS defective virus causes expansion of its target cells are unknown. The defective viral genome does not harbor an oncogene and appears to encode a single protein, the $Pr60^{gag}$ precursor (2, 10, 25). This protein and its location on cell membranes seem necessary and sufficient for the virus to induce rapid expansion of infected target cells (24, 26, 51). Initially, this proliferation is polyclonal, but it is clonal or oligoclonal in late stages of the disease (29). The oligoclonality of the infected target cell population observed late in the disease suggests that additional secondary genetic events occur in some infected cells and give them a growth advantage, possibly cooperating with $Pr60^{gag}$.

For many MuLVs, the activation of cellular proto-oncogenes by provirus integration constitutes an important step in the tumorigenic process (for reviews, see references 36 and 46). By acting as an insertional mutagen, the provirus can activate gene expression, decrease transcription, or alter gene structure, thus providing a growth advantage for the target cells. Many cellular DNA regions have been identified as common MuLV provirus integration sites, and their rearrangements were found to be involved in the development of virus-induced T-cell leukemia and B-cell lymphomas (36, 46).

The same strategy of insertional mutagenesis may be used by the MAIDS defective virus to favor the growth of some infected cells. To determine whether the integration of the MAIDS defective viral genome into particular chromosomal regions contributes to the oligoclonal expansion of infected target cells, we searched for common provirus integration sites in enlarged lymphoid organs of MAIDS mice at a late stage of the disease. Here we report the identification of two common MAIDS provirus integration sites. Our results suggest that in addition to coding for $Pr60^{gag}$, the MAIDS defective viral genome acts as an insertional mutagen in infected target cells.

MATERIALS AND METHODS

Animals and viruses. Inbred C57BL/6 mice were purchased from Charles River Inc. (St-Constant, Québec, Canada) and housed in the same room during

* Corresponding author. Mailing address: Laboratory of Molecular Biology, Clinical Research Institute of Montreal, 110 Pine Ave. West, Montréal, Québec, Canada H2W 1R7. Phone: (514) 987-5569. Fax: (514) 987-5794.

† Present address: Institute of Molecular Genetics, Academy of Sciences of the Czech Republic, 166 37 Praha 6, Czech Republic.

the experiments. Young (30- to 40-day-old) mice were inoculated with helper-free stocks of MAIDS defective virus Du5H/Mo-LTR as described previously (29). Splenomegaly and lymphadenopathy developed 3 to 5 months postinoculation. Mice were sacrificed, and the enlarged lymphoid organs were then used for further analysis.

DNA extraction and restriction endonuclease digestion. High-molecular-weight cellular DNAs were prepared from the enlarged lymphoid organs as previously described (29, 48). They were digested with various restriction endonucleases (New England Biolabs, Inc., Beverley, Mass.; Boehringer Mannheim Biochemicals, Montréal; Québec, Canada; and P-L Pharmacia, Montreal, Québec, Canada) under conditions recommended by the manufacturers, as previously described (38, 39). Bacteriophage and plasmid DNAs were prepared essentially as described elsewhere (39).

Agarose gel electrophoresis and hybridization procedure. Digested DNA samples were electrophoresed on 1% agarose gels and transferred onto nitrocellulose or nylon membranes (Amersham Co., Montréal, Québec, Canada) by the Southern technique (61), as described previously (38, 39, 48). Specific DNA fragments were detected by hybridization with ^{32}P-labeled cloned DNA fragments. These cloned DNA fragments were excised from vectors and separated by agarose gel electrophoresis. DNA fragments were isolated by electroelution onto NA45 affinity paper (Schleicher & Schuell), phenol-chloroform extracted, and precipitated with ethanol, as described previously (48). Probes were labeled by the random priming method with the Klenow fragment of DNA polymerase I in the presence of hexamers (16). Nitrocellulose filters were hybridized in 50% formamide–3× SSC (1× SSC is 0.15 M NaCl plus 0.015 M sodium citrate)–Denhardt solution at 42°C. Nylon membranes were hybridized in 4× SET (1× SET contains 0.15 M NaCl, 30 mM Tris, and 2 mM EDTA, pH 7.4) with 0.1% sodium PP_i–0.2% sodium dodecyl sulfate (SDS)–10% dextran sulfate–0.5 mg of heparin per ml at 65°C for 16 h. After hybridization, all membranes were washed in 2× SSC for 15 min at room temperature, 0.1× SSC–0.1% SDS for 1 h at 65°C, and three times, for 2 min each time, in 0.1× SSC at room temperature. Membranes were air dried and exposed on RP-Royal X-Omat film (Eastman Kodak Co., Rochester, N.Y.) with a Cronex Lightning-Plus intensifying screen (DuPont Co., Wilmington, Del.) at −70°C.

Molecular cloning procedure. DNAs E20-1-7 and E1-2-6 from enlarged lymph nodes of MAIDS mice were digested with *Eco*RI and *Bam*HI, respectively, and centrifuged on a sucrose density gradient (10 to 40%) as previously described (38, 49, 66). Fractions of 0.5 ml were collected and ethanol precipitated. Aliquots of DNA from each fraction were separated by agarose gel electrophoresis, transferred onto a nylon membrane, and hybridized with a Moloney MuLV U3 long terminal repeat (LTR)-specific probe (29). Fractions containing 5- to 20-kbp viral fragments were pooled and ligated with *Eco*RI-cleaved EMBL-4 or *Bam*HI-cleaved EMBL-3 arms. The ligated DNAs were packaged with Gigapack extracts (Stratagene) as described elsewhere (38, 39). Recombinant phages harboring Du5H/Mo-LTR sequences were identified with the ^{32}P-labeled Moloney MuLV-U3 LTR-specific probe. Phages were eluted, and their DNA was extracted on a double 5 and 40% glycerol cushion. Inserts were subcloned into plasmid vectors as described elsewhere (39, 49, 66).

Probes. The Moloney MuLV U3 LTR-specific probe consists of a 0.3-kbp *Pst*I-*Sac*I fragment from a mutated Moloney MuLV LTR (48, 49, 55). The probes specific for the c-*myc* (37), *Vin-1* (62), *Pal-1* (64), *Myb* (21), *Pim-1* (14), *Ahi-1* (49), *Bmi-1* (64), *Evi-2* (6), *Spi-1* (45), *Erb-A* (65), *Erb-B2* (3), and *Csfg* genes and *Spi-1* cDNA (41) have been described elsewhere.

RNA expression analysis. RNA was isolated from various tissues by the method of Chomczynski and Sacchi (13), separated on 1% formaldehyde-agarose gels, transferred onto nylon membranes, and hybridized as described above. Washings were performed for 15 min at room temperature in 2× SSC, for 1 h at 65°C in 0.1× SSC–0.1% SDS, and three times, for 2 min each time, at room temperature in 0.1× SSC.

Genetic crosses. Two multilocus genetic crosses were analyzed to map Dis-1 and Dis-2: (NFS/N or C58J × *Mus musculus* subsp. *musculus*) × *M. musculus* subsp. *musculus* (35) and (NFS × *M. spretus*) × *M. spretus* or C58/J (1). DNAs from the progeny of these crosses have been typed for approximately 700 markers which map to all 19 autosomes and the X chromosome. Blot transfer methods and hybridization probes have been previously described for the following markers on chromosome 2: *Sfpi1* (spleen focus-forming virus proviral integration Spi-1/PU.1), *Mtap1* (microtubule-associated protein 1), *B2m* (β-2 microglobulin), *Cyct* (cytochrome *c*, testis), *Gad1* (glutamic acid decarboxylase 1), and *Hgm1* (HMG box protein gene 1) (1, 9, 23, 47). We also typed the following chromosome 11 markers as described previously: *Scya2* (small inducible cytokine a2, formerly *Sigje*), *Scya6* (small inducible cytokine a6), *Fkbprp* (FK506 binding protein), *Evi-2* (ecotropic viral integration site 2), *Hox2* (homeobox 2 cluster), *Erb-B2* (avian erythroblastosis virus oncogene B-2), and *Wnt3* (*wingless*-related mouse mammary tumor virus integration site, formerly *Int-4*) (5, 34, 60).

Data were stored and analyzed by using the program LOCUS. Percent recombination and standard errors between specific loci were calculated from the number of recombinants as described by Green (22). Loci were ordered by minimizing the number of double recombinants.

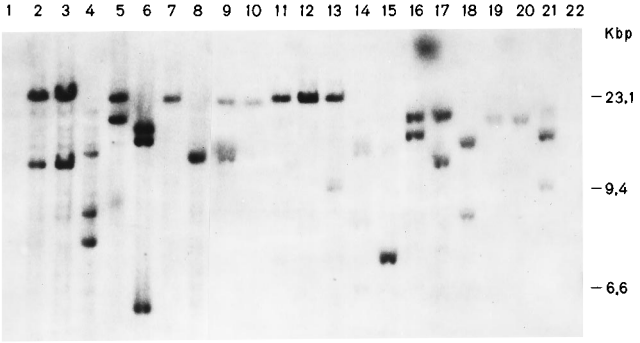

FIG. 1. Southern blot analysis of proviruses present in enlarged lymphoid organs of MAIDS mice. DNAs (20 μg) from normal organs (lanes 1 and 22) and from enlarged spleens and lymph nodes (lanes 2 to 21) were digested with *Bam*HI (lanes 1 to 8) or *Eco*RI (lanes 9 to 22), electrophoresed on 1% agarose gels, transferred to nitrocellulose membranes, and hybridized with a Moloney MuLV U3 LTR-specific probe. Lanes 2 and 3, 9 and 10, 11 to 13, 14 and 15, 16 to 18, and 19 and 20 are different nodes from the same mouse.

RESULTS

Analysis of proviruses in lymphoid cells infected with MAIDS defective virus Du5H/Mo-LTR. Helper-free stocks of molecularly cloned MAIDS defective virus Du5H/Mo-LTR induce the clonal proliferation of infected B cells in 100% of inoculated C57BL/6 mice after a relatively short latency period (2 to 6 months). This virus was constructed by exchanging the U3 LTR region of the wild-type MAIDS defective viral genome for the U3 LTR region of the Moloney MuLV (29). This modification allowed its specific detection with a Moloney MuLV U3 LTR-specific probe. To analyze the structure of the Du5H/Mo-LTR defective proviruses in clonally expanded infected B cells, spleen and lymph node DNAs from MAIDS mice inoculated with this virus were first analyzed by restriction endonucleases with the Moloney MuLV U3 LTR-specific probe.

We chose *Eco*RI and *Bam*HI for this analysis, as neither of these enzymes cleaves the Du5H/Mo-LTR defective viral genome, thus allowing detection of newly acquired Du5H/Mo-LTR proviruses flanked by cellular sequences. In all of the tumors screened, newly acquired proviruses could be detected by hybridization with the Moloney MuLV U3 LTR-specific probe (Fig. 1). The presence of discrete bands in all of the samples indicated that the proliferation of the cells infected with the MAIDS defective virus was clonal or oligoclonal in origin. The distinct patterns of provirus integration often seen in different organs of the same animal indicated that a single animal may carry multiple independent clones of tumor cells. These observations confirmed our previous results (29). In each individual sample, the number of newly acquired proviruses was relatively small and varied from one to three, in contrast to the large number of proviruses normally detected in T-cell tumors induced by various MuLVs (38, 62, 66).

To study the role of insertional mutagenesis by Du5H/Mo-LTR proviruses in the clonal proliferation of these infected B cells, we first screened a series of infiltrated organ DNAs by using probes specific for various oncogenes which have been reported to be activated by provirus insertions. Probes detecting c-*myc*, *Vin-1*, *Pal-1*, c-*myb*, *Pim-1*, *Ahi-1*, *Bmi-1*, and *Evi-2* were used on 15 DNAs from different mice, all of which exhibit distinct viral integration patterns. These DNAs were digested with restriction enzymes *Eco*RV, *Bam*HI, and *Kpn*I to screen a relatively large DNA fragment so that in most cases, a proviral insertion close to the oncogene screened would generate a

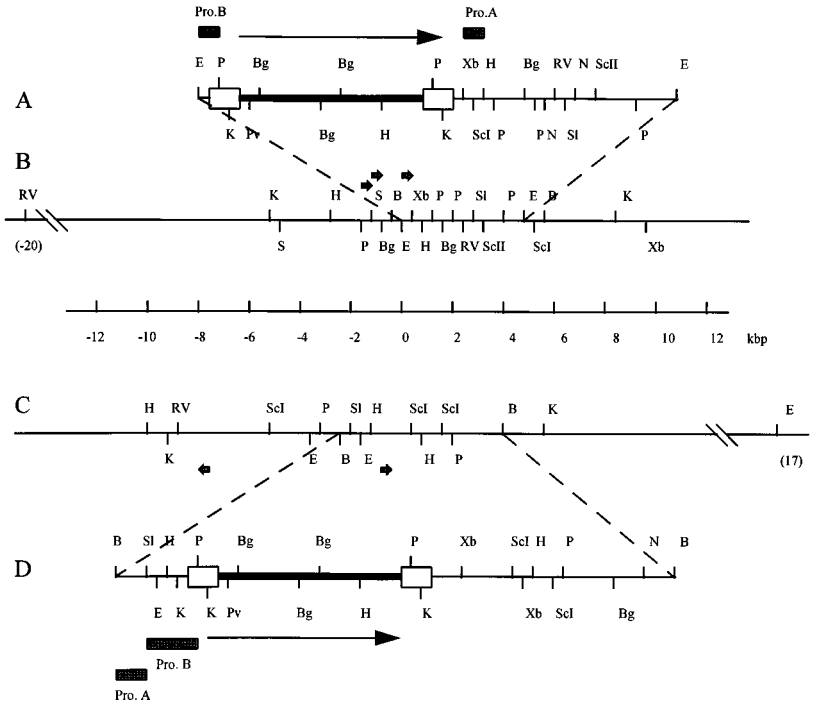

FIG. 2. Restriction endonuclease map of the Dis-1 and Dis-2 loci. (A) Schematic representation of the provirus inserted within the Dis-1 locus and cloned from MAIDS DNA E20-1-7. (B) Diagram of a normal C57BL/6 mouse Dis-1 locus with the locations of the MAIDS defective proviruses found in this region. (C) Diagram of the Dis-2 locus with the locations of the MAIDS defective proviruses found in this region. (D) Schematic representation of the provirus inserted within the Dis-2 locus and cloned from MAIDS DNA E1-2-6. The arrows show the transcriptional orientation of the proviruses, the thick lines represent viral sequences, the open boxes are retroviral LTRs, and the closed boxes are probes (Pro.). Restriction sites: B, *Bam*HI; Bg, *Bgl*II; E, *Eco*RI; H, *Hin*dIII; K, *Kpn*I; N, *Nhe*I; P, *Pst*I; Pv, *Pvu*I; RV, *Eco*RV; S, *Sma*I; Sc, *Sac*I; ScII, *Sac*II; S1, *Sal*I; X, *Xho*I; Xb, *Xba*I.

smaller rearranged fragment, which could then be detected easily. Among the 15 DNAs screened, only one showed a rearranged *Kpn*I fragment with the c-*myc* probe (data not shown). The rearranged fragment was about 12 to 13 kbp long, 3 to 4 kb larger than the unrearranged germ line fragment. Since *Kpn*I cuts the viral genome twice in the LTR R region, insertion of the provirus into this region should have generated a rearranged fragment shorter than the germ line fragment. Therefore, this rearrangement very likely reflects an event unrelated to Du5H/Mo-LTR insertion. The nature of this rearrangement was not investigated further. Therefore, it appears that many of the oncogenes which have been found to be activated by provirus insertion in other MuLV-induced tumors are not targetted by the MAIDS defective provirus.

Cloning of virus-cell junction fragments in lymphoid cells infected with MAIDS defective virus Du5H/Mo-LTR. To further study the role of insertional mutagenesis by Du5H/Mo-LTR proviruses in the clonal outgrowth of infected B cells, the Du5H/Mo-LTR proviruses flanked by their adjacent cellular sequences were cloned from two individual organs. Enlarged lymph nodes E20-1-7 and E1-2-6 from two independent diseased mice were chosen because they contain a small number (two for E20-1-7 and one for E1-2-6) of easily detectable, newly acquired proviral *Eco*RI (E20-1-7) (29) and *Bam*HI (E1-2-6) (Fig. 1, lane 8) fragments of about 10 to 15 kbp. The size-selected *Eco*RI and *Bam*HI fragments from the DNAs of these organs were ligated to EMBL-4 and EMBL-3 phage arms, respectively, and cloned. Recombinant phages were identified with the ^{32}P-labeled Moloney MuLV U3 LTR-specific probe.

One of the two detectable *Eco*RI fragments from DNA E20-1-7 and the single *Bam*HI fragment from DNA E1-2-6 containing viral sequences were successfully cloned, as judged by comigration of *Eco*RI- and *Bam*HI-cleaved cloned proviral DNAs with proviruses of DNAs from corresponding tumors cleaved with the same enzymes (data not shown). The cloned proviruses from DNAs E20-1-7 and E1-2-6 were then subcloned into plasmid pBR322 and analyzed by restriction endonuclease digestions and Southern blotting with the Moloney MuLV U3 LTR-specific probe. Both of them were found to represent complete Du5H/Mo-LTR genomes (data not shown).

Cellular fragments adjacent to each provirus were subcloned, and those free of repetitive sequences were used as probes to screen other DNAs from infiltrated MAIDS organs to search for common proviral integration sites. By using one of these probes (probe A), derived from one cloned provirus from DNA E20-1-7, we were able to identify rearrangements in DNAs of other organs from different animals with MAIDS (see below). This region, which represents a common proviral integration site, was designated Dis-1 (Du5H integration site 1). Similarly, probe B, derived from the cloned provirus from DNA E1-2-6, also disclosed a common proviral integration site different from Dis-1 (see below). This region was designated Dis-2.

Molecular characterization of the Dis-1 and Dis-2 regions. Crude restriction maps of the Dis-1 and Dis-2 regions were obtained by digestion of healthy C57BL/6 mouse cellular DNA with various restriction endonucleases, alone or in combination, and hybridization with Dis-1 probe A or Dis-2 probe A and/or probe B (data not shown). A summary of these data is presented in Fig. 2. This analysis allowed us to select appropriate restriction endonucleases to screen for new rearrangements in these regions by using tumor DNAs from other diseased mice, as well as to map more precisely the integration

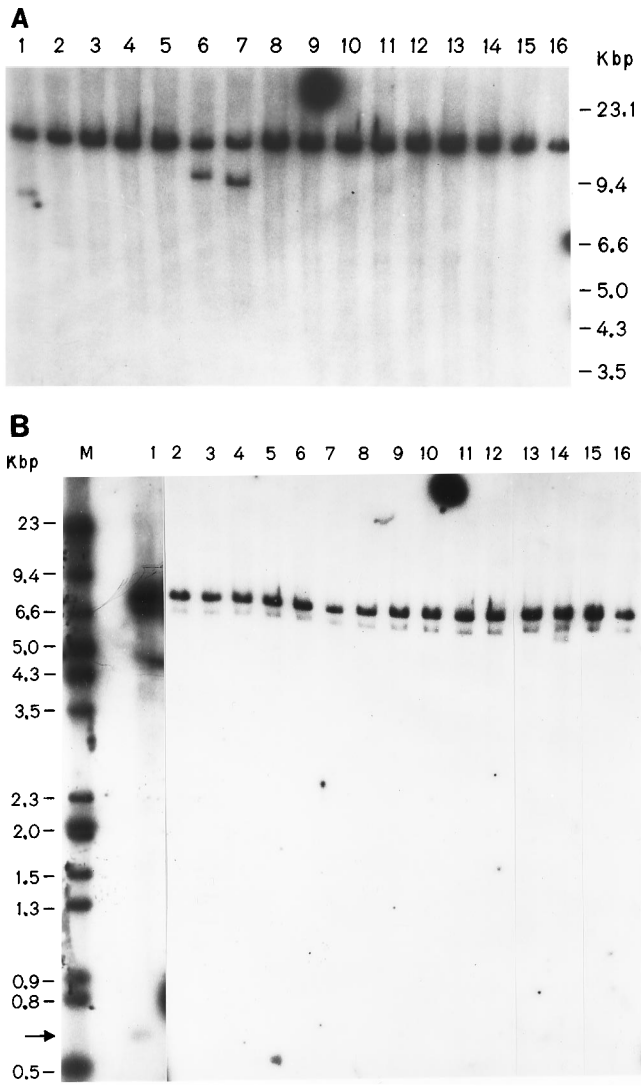

FIG. 3. Southern blot analysis of DNAs from enlarged organs of MAIDS mice. Probes specific to the Dis-1 (A) and Dis-2 (B) regions were used. (A) *Kpn*I-digested DNAs (20 μg) from 15 MAIDS-enlarged spleens or lymph nodes (lanes 1 to 15) were screened with Dis-1 probe A. Lane 16 is DNA from the spleen of a healthy, uninoculated C57BL/6 mouse. (B) *Kpn*I-digested DNAs (20 μg) from the same 15 MAIDS organs (lanes 1 to 15, not in the same order as in panel A) were screened with Dis-2 probe B. Lane 16 is DNA from the spleen of a healthy, uninoculated mouse. Lane 1 is a longer exposure done to reveal the 0.7-kbp band (arrow).

sites of each provirus found within these regions, and as it turned out later, to compare these regions with other candidate regions which have been identified previously.

Detection of proviruses integrated within the Dis-1 or Dis-2 region in B cells infected by the MAIDS defective virus. To determine the frequency at which defective virus Du5H/Mo-LTR integrated into the Dis-1 or Dis-2 region in other DNAs from organs of animals with MAIDS, we first screened 15 of these *Kpn*I-digested DNAs by the Southern technique using ^{32}P-labeled Dis-1 probe A. *Kpn*I was chosen because a relatively long region (about 13 kbp) could be screened with probe A and because it cleaves within the LTR of the defective virus. Three tumors (20%), including the original one, had a novel tumor-specific fragment in addition to the germ line fragment of the normal allele (Fig. 3A, lanes 1, 6, and 7). The same set of tumors was also screened with Dis-2 probe B. This probe is a 0.8-kbp *Sal*I-*Pst*I DNA fragment derived from a cellular sequence exactly adjacent to the 5′ LTR of integrated provirus in tumor E1-2-6. *Kpn*I cuts the probe once and therefore gave two germ line fragments of about 7.2 and 8 kbp surrounding the provirus integration site in the original tumor (Fig. 3B, lane 1). In addition to the rearranged fragment detected in the original tumor (E1-2-6) (Fig. 3B, lane 1), *Dis2* probe B detected a novel tumor-specific fragment in another tumor (E1-4-6; Fig. 3B, lane 14).

Therefore, both Dis-1 and Dis-2 represent common proviral integration sites in cells infected with the MAIDS defective virus. The number of tumors screened is relatively small, so the frequencies at which these regions were occupied by proviruses appear relatively high (20% for Dis-1 and 13% for Dis-2) and very significant, considering the low probability of two independent proviral integration events occurring at random in the same 13- to 15-kbp genomic fragment.

Structural organization of defective proviruses within the Dis-1 and Dis-2 regions. Rearrangements of a given DNA region within the genome of a tumor cell can arise by different molecular mechanisms. To determine whether the rearrangements detected with *Kpn*I within the Dis-1 and Dis-2 regions indeed reflected the integration of MAIDS defective provirus Du5H/Mo-LTR, to map each of them more precisely, and to identify their transcriptional orientation, we performed a restriction analysis of the organ DNAs where rearrangements were found.

Dis-1 probe A detected a 13-kbp *Kpn*I germ line fragment in normal tissues. Additional *Kpn*I fragments of about 7.5, 9.5, and 9 kbp were detected in organ DNAs E20-1-7, E20-3-1, and E20-4-1, respectively (Fig. 3A, lanes 1, 6, and 7), suggesting the presence of a provirus in the Dis-1 region of these DNAs, thus introducing a *Kpn*I site within the 13-kbp germ line fragment. As the cloned integrated provirus in the original E20-1-7 organ was mapped precisely, we completed this analysis for the other two organ DNAs, E20-3-1 and E20-4-1, with restriction enzymes *Kpn*I-*Eco*RV, *Eco*RV, *Pst*I, and *Hin*dIII (Fig. 4A). In DNAs from healthy C57BL/6 mice, Dis-1 probe A detected a single *Eco*RV fragment of about 23 kbp, while novel fragments of 4.3 and 3.8 kbp were detected in DNAs E20-3-1 and E20-4-1, respectively. With *Pst*I, Dis-1 probe A detected a novel 3.2-kbp fragment (in addition to the 2.7-kbp germ line fragment) in E20-3-1 DNA, while no clearly distinct novel fragment was detectable from E20-4-1 DNA. With *Hin*dIII, probe A detected a novel 3.9-kbp fragment and a novel 3.4-kbp fragment in the E20-3-1 and E20-4-1 DNAs, respectively, in addition to the 3.5-kbp germ line fragment. These results are consistent with the presence of a Du5H/Mo-LTR provirus integrated upstream of Dis-1 probe A in organ DNAs E20-3-1 and E20-4-1 and about 1.3 to 1.8 kbp upstream of the provirus integration site in the original tumor, E20-1-7. This analysis also allowed determination of the provirus orientation. The presence of a novel *Hin*dIII site at about 1.1 kbp upstream from the novel *Eco*RV and *Pst*I sites is consistent with the presence of a Du5H/Mo-LTR provirus (which harbors *Hin*dIII, *Eco*RV, and *Pst*I sites in the middle of the genome [*Hin*dIII] or in the LTR region [*Eco*RV and *Pst*I], respectively) oriented toward probe A in the Dis-1 region. Furthermore, when DNAs E20-3-1 and E20-4-1 were double digested with *Kpn*I and *Eco*RV, the novel fragments (Fig. 4A, lanes 1 and 9) were about 0.3 kbp shorter than the corresponding novel fragments from the same samples digested by *Eco*RV alone (Fig. 4A, lanes 2 and 10). Since a *Kpn*I site is located ~300 bp downstream of the *Eco*RV site in the proviral LTR, these results further confirmed the orientation of the provirus in

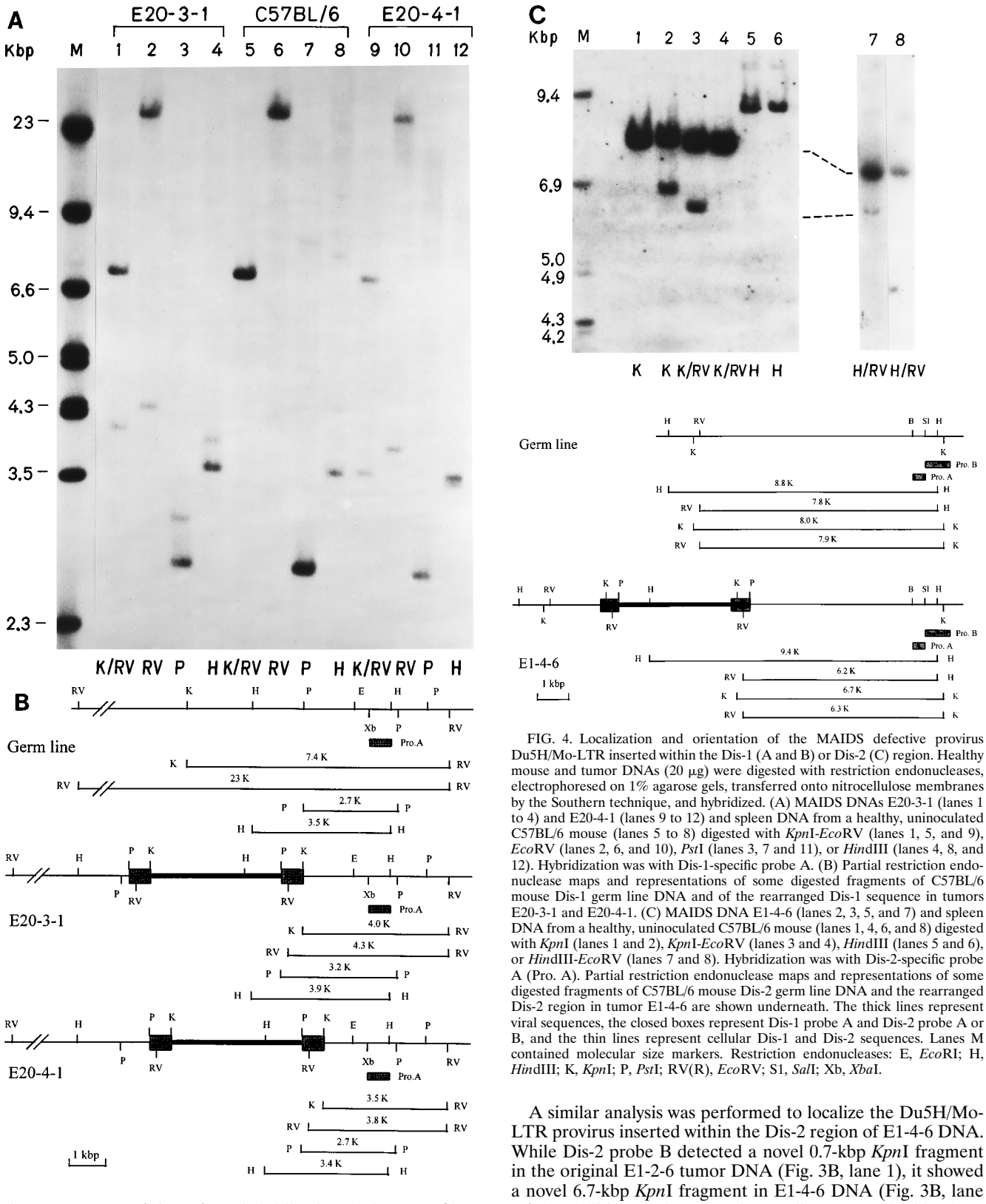

FIG. 4. Localization and orientation of the MAIDS defective provirus Du5H/Mo-LTR inserted within the Dis-1 (A and B) or Dis-2 (C) region. Healthy mouse and tumor DNAs (20 μg) were digested with restriction endonucleases, electrophoresed on 1% agarose gels, transferred onto nitrocellulose membranes by the Southern technique, and hybridized. (A) MAIDS DNAs E20-3-1 (lanes 1 to 4) and E20-4-1 (lanes 9 to 12) and spleen DNA from a healthy, uninoculated C57BL/6 mouse (lanes 5 to 8) digested with *Kpn*I-*Eco*RV (lanes 1, 5, and 9), *Eco*RV (lanes 2, 6, and 10), *Pst*I (lanes 3, 7 and 11), or *Hin*dIII (lanes 4, 8, and 12). Hybridization was with Dis-1-specific probe A. (B) Partial restriction endonuclease maps and representations of some digested fragments of C57BL/6 mouse Dis-1 germ line DNA and of the rearranged Dis-1 sequence in tumors E20-3-1 and E20-4-1. (C) MAIDS DNA E1-4-6 (lanes 2, 3, 5, and 7) and spleen DNA from a healthy, uninoculated C57BL/6 mouse (lanes 1, 4, 6, and 8) digested with *Kpn*I (lanes 1 and 2), *Kpn*I-*Eco*RV (lanes 3 and 4), *Hin*dIII (lanes 5 and 6), or *Hin*dIII-*Eco*RV (lanes 7 and 8). Hybridization was with Dis-2-specific probe A (Pro. A). Partial restriction endonuclease maps and representations of some digested fragments of C57BL/6 mouse Dis-2 germ line DNA and the rearranged Dis-2 region in tumor E1-4-6 are shown underneath. The thick lines represent viral sequences, the closed boxes represent Dis-1 probe A and Dis-2 probe A or B, and the thin lines represent cellular Dis-1 and Dis-2 sequences. Lanes M contained molecular size markers. Restriction endonucleases: E, *Eco*RI; H, *Hin*dIII; K, *Kpn*I; P, *Pst*I; RV(R), *Eco*RV; S1, *Sal*I; Xb, *Xba*I.

these two tumors (Fig. 4B). Rehybridization of the same filter with the Moloney MuLV U3 LTR-specific probe (data not shown) confirmed that the newly acquired Dis-1 probe A-hybridizing *Eco*RV, *Pst*I, or *Hin*dIII fragments from these two organs all contain Moloney MuLV LTR sequences.

A similar analysis was performed to localize the Du5H/Mo-LTR provirus inserted within the Dis-2 region of E1-4-6 DNA. While Dis-2 probe B detected a novel 0.7-kbp *Kpn*I fragment in the original E1-2-6 tumor DNA (Fig. 3B, lane 1), it showed a novel 6.7-kbp *Kpn*I fragment in E1-4-6 DNA (Fig. 3B, lane 14), in addition to the normal germ line 7.2- and 8-kbp fragments. Since probe B detected two *Kpn*I fragments, the 6.7-kbp rearranged fragment could be derived from either of them (Fig. 2) and the provirus in this tumor could be integrated on either side of this *Kpn*I site. However, when the DNA was

double digested with *Hin*dIII and *Eco*RV and hybridized with another probe, Dis-2 probe A (which is a 0.5-kbp cellular fragment just upstream of Dis-2 probe B), a novel fragment could still be detected (Fig. 4C, lane 7), indicating that the integration site of this provirus was upstream of the probe B *Kpn*I site, namely, in the longer *Kpn*I fragment detected by probe B. Thus, on the basis of results obtained with probe B, the provirus either was integrated about 6.2 kbp upstream of the probe B *Kpn*I site and is oriented away from probe B or was integrated 6.6 kbp upstream of the *Kpn*I site and is oriented toward probe B. To locate it more precisely, the DNAs were digested with *Kpn*I alone or with *Kpn*I and *Eco*RV and then hybridized with Dis-2 probe A. In sample E1-4-6, a novel 6.7-kbp *Kpn*I fragment was detected (Fig. 4C, lane 2), while *Kpn*I-*Eco*RV double digestion of this sample resulted in a 6.3-kbp fragment which also hybridized with this probe (Fig. 4C, lane 3). Since the *Eco*RV sites are located at the 5′ region upstream of the *Kpn*I site in the viral LTR, this result indicated that the provirus was inserted 6.2 kbp upstream of the probe B *Kpn*I site and is oriented away from probe B. In agreement with this, the novel *Hin*dIII-*Eco*RV fragment of E1-4-6 DNA, which hybridized with probe A, was about 6.2 kbp long (Fig. 4C, lane 7). The opposite orientation of an inserted provirus would have given rise to a 6.9-kbp fragment. This result was further confirmed by using Dis-2 probe A on E1-4-6 DNA digested with *Hin*dIII alone. A novel and faint 9.4-kbp fragment was detected in addition to the 8.8-kbp germ line fragment (Fig. 4C, lane 5). Had the provirus been integrated at the other putative site, as described above, the faint rearranged fragment would have been 1.3 kbp smaller.

Interestingly, the three proviruses detected within the Dis-1 region were all inserted in the same transcriptional orientation, while the two proviruses in the Dis-2 region were inserted in opposite directions.

Dis-1 maps to murine chromosome 2, and Dis-2 maps to murine chromosome 11. The chromosome locations of Dis-1 and Dis-2 were established by analysis of the progeny of two multilocus crosses. For Dis-1, DNAs of parental NFS/N and *M. musculus* subsp. *musculus* mice produced *Xba*I fragments of 8.7 and 8.4 kb, respectively. Digestion with *Bgl*II produced an NFS/N fragment of 2.7 kb and an *M. spretus* fragment of 3.0 kb. For Dis-2, *Eco*RI fragments of 2.3 and 25.0 kb were identified in NFS/N and *M. musculus* subsp. *musculus* DNAs, respectively, and *Pvu*II fragments of 2.5 and 3.2 kb were detected in NFS and *M. spretus* DNAs. Progeny of both crosses were typed for inheritance of the polymorphic fragments, and the inheritance patterns were compared with inheritance of approximately 700 markers previously typed and mapped in these crosses. Results indicated that Dis-1 maps to mouse chromosome 2 at or near the previously described preferred viral integration site, *Sfpi1*. No recombinants were detected in the 176 mice typed for Dis-1 and *Sfpi1*. This indicates that, at the 95% confidence level, these genes are within 1.7 centimorgans.

Examination of the inheritance of Dis-2 in both crosses indicated that it maps to a region of chromosome 11 which contains a number of genes which have been implicated in oncogenesis, including *Evi-2*, *Erb-B2*, *Erb-A*, *Csfg*, and *Ngfr*. The progeny of one or both of our crosses were typed for *Evi-2* and *Erb-B2*, as well as the more distal locus *Wnt3*. In all cases, we identified recombinants between Dis-2 and each of these loci, indicating that none of these genes is a candidate for Dis-2. The map location of Dis-2 proximal to *Hox2* further indicates that Dis-2 is distinct from the *Erb-A* and *Csfg* loci, which have been positioned distal to *Hox2* (7). Furthermore, our data show that Dis-2 is about 9 centimorgans from *Hox2*.

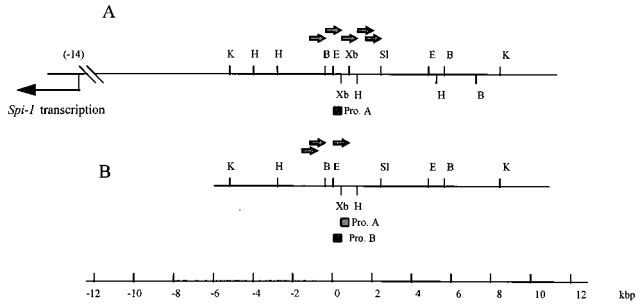

FIG. 5. Comparison of partial restriction maps of the Spi-1 (A) and Dis-1 (B) regions. The map of Spi-1 is taken from reference 45. For the Dis-1 region, only the restriction sites relevant for this comparison are shown. Figure 2 contains a detailed map of Dis-1. Probes (Pro.) specific for the Spi-1 and Dis-1 regions are shown as closed boxes. The thick arrows indicate sites of provirus integrations in spleen focus-forming virus-induced erythroleukemias (Spi-1) or MAIDS B cells (Dis-1) and the 5′-to-3′ orientation of the provirus.

Since the *Hox2* cluster and *Ngfr* are located within a <150-kbp region (4), we conclude that Dis-2 is also distinct from *Ngfr*.

In further studies, DNAs from C57BL/6 mice were digested by *Eco*RI or *Hin*dIII and hybridized with probes specific for the *Erb-A*, *Erb-B2*, and *Csfg* genes. We found that the lengths of the fragments hybridizing with these probes were different from those of Dis-2 (data not shown), also suggesting that Dis-2 is distinct from either of these loci. Therefore, Dis-2 appears to be a novel gene likely to be involved in the proliferation of B cells infected by the MAIDS defective virus.

The Dis-1 region corresponds to the Spi-1/PU.1 locus. Since the linkage analysis indicated that Dis-1 was very close to the Spi-1 locus, it was of interest to compare the genomic organization of the Dis-1 and Spi-1 regions and their possible identity. Spi-1 was initially identified as a common proviral integration site in spleen focus-forming virus-induced murine erythroleukemias (42, 45) and later found also to be involved in other erythroleukemias (40). We first compared the restriction maps of these two regions. The restriction endonuclease map of Dis-1 was very similar to the reported map of the Spi-1 region, although some differences were observed (Fig. 5). This suggested the identity of Dis-1 with an area 15 kbp upstream of the protein-encoding domain of the Spi-1 gene. To confirm this identity, we used a 0.3-kbp *Eco*RI-*Sac*I Spi-1 DNA fragment specific for DNA sequences 14 to 15 kbp upstream of the Spi-1 coding region (Fig. 5A) as a probe (Spi-1 probe A) (45) to hybridize to the Dis-1 cloned DNA fragment. We found that both Dis-1 probe A (Fig. 5 shows the location) and the cloned Dis-1 fragment (Fig. 2A) digested by several restriction enzymes could all be detected with Spi-1 probe A in Southern blot analysis, as expected (data not shown), indicating the relatedness of these sequences. Furthermore, the Spi-1-specific probe was used to screen the same 15 organ DNAs from MAIDS animals previously screened with the Dis-1 probe (Fig. 3A). The three organs showing Dis-1 rearrangements also showed rearrangements when the Spi-1 probe was used (Fig. 6). Together, these results indicated that the Dis-1 region corresponds to the Spi-1 locus.

Dis-1–Spi-1 RNA expression is increased in organs exhibiting rearrangement within the Dis-1–Spi-1 locus. Provirus integration within the Spi-1 locus has previously been reported to increase expression of the Spi-1 gene (41, 42). To determine whether integration of this Du5H/Mo-LTR defective MAIDS provirus also affects Spi-1 gene expression, we extracted total RNAs from various MAIDS organs, including some with and some without DNA rearrangements in the Dis-1–Spi-1 locus,

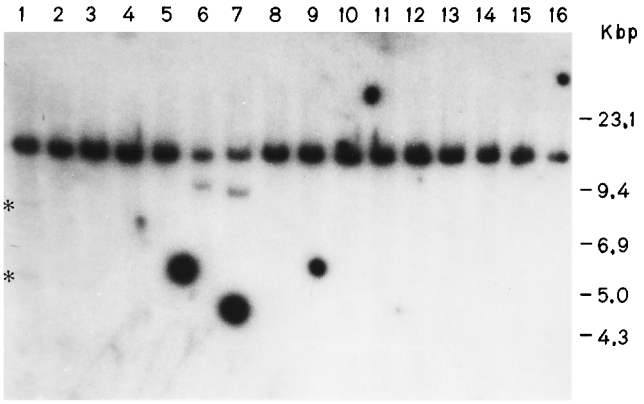

FIG. 6. Detection of rearrangements with the Spi-1 and Dis-1 probes. The filter shown in Fig. 3A, containing 15 DNAs from MAIDS organs, was washed and rehybridized with Spi-1-specific probe A. The three DNAs which show a rearrangement within Spi-1 (lanes 1, 6, and 7) also showed a rearrangement in the Dis-1 region (Fig. 3A). The asterisks indicate the faint rearranged bands in lane 1.

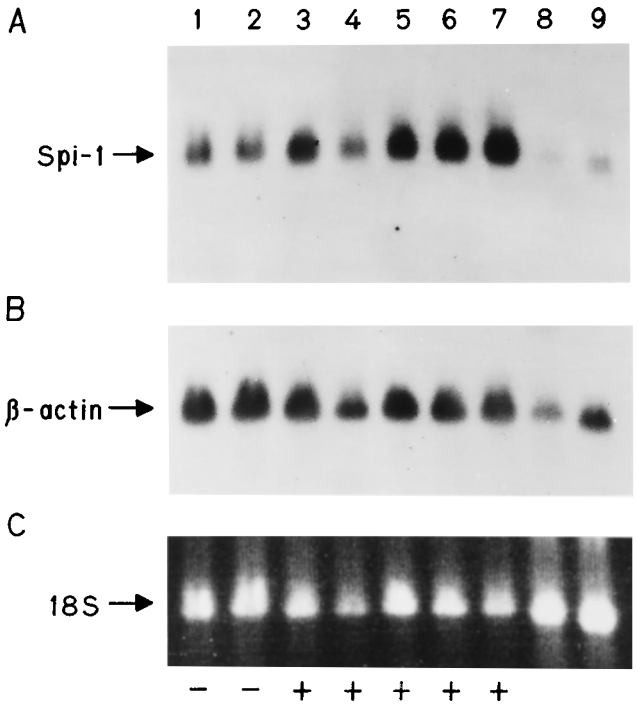

FIG. 7. Overexpression of Spi-1 RNA in MAIDS organs exhibiting rearrangement in the Dis-1–Spi-1 region. Total RNAs (20 μg) were extracted from spleens of healthy C57BL/6 mice (lanes 8 and 9) and from enlarged spleens or lymph nodes of MAIDS mice with (+) (lanes 3 to 7) or without (−) (lanes 1 and 2) rearrangement within the Dis-1–Spi-1 locus. The RNAs were separated on formaldehyde-agarose gels, transferred onto nitrocellulose membranes, and hybridized with a ^{32}P-labeled Spi-1 cDNA probe (41) (A). The same filter was then washed and rehybridized with a β-actin probe (B). The ethidium bromide staining of 18S rRNA of the same gel is shown in panel C. Lanes 3 and 4 and lanes 5 and 6 are RNAs of two different organs of the same mouse.

and hybridized these with a Spi-1 cDNA probe (41). Spi-1 expression was weak in spleens of healthy, uninoculated mice (Fig. 7, lanes 8 and 9). The expression was clearly increased in all of the infiltrated MAIDS mouse organs screened. However, in all five organs from three diseased MAIDS mice which showed provirus insertion within the Dis-1–Spi-1 region, the levels of Spi-1 RNA were two to three times higher (Fig. 7, lanes 3 to 7) than those of organs without proviral insertion in this region (Fig. 7, lanes 1 to 2). This result suggested that Spi-1 expression was upregulated as a result of MAIDS defective provirus integration upstream of this oncogene.

DISCUSSION

MAIDS defective proviruses act as insertion mutagens. We have previously reported that the lymphoid cells infected by the MAIDS defective virus in enlarged lymphoid organs of diseased mice represent oligoclonal proliferation (27, 29). This result suggested that secondary genetic events, in addition to the Pr60^{gag} viral protein, contributed to this oligoclonal outgrowth. In the present study, we investigated whether the MAIDS defective provirus acts as an insertional mutagen to participate in the proliferation of infected target cells. Insertional mutagenesis by proviruses has previously been shown to be an important mechanism of oncogenesis in tumors induced by several different replication-competent MuLVs (36, 46). As with proviruses from replicating helper MuLVs, two common defective proviral integration sites (Dis-1 and Dis-2) were identified in enlarged organs of MAIDS-diseased mice. The frequencies of provirus occupancy of these loci are not very high (20% for Dis-1 and 13% for Dis-2). However, the chance of two random integration events occurring in a 30-kbp region is only about 10^{-10} (46). Although factors like nucleosomes, DNA-binding proteins, and DNA sequences may modulate retroviral integration target site selection and result in some "hot spots" for the insertion (20, 52), these factors are unlikely to explain the phenomenon observed here, since identification of Dis-1 and Dis-2 was done in cells which showed a selective growth advantage. While Dis-2 appears to be a novel locus possibly harboring a gene involved in cell proliferation, the Dis-1 locus was found to represent the proto-oncogene *Sfpi1* (Spi-1/PU.1) locus. As shown by our data, c-*myc* was not found to be a frequent target for the MAIDS defective provirus in organs of diseased mice inoculated with the helper-free MAIDS defective virus. A similar observation was made by Klinken et al. (33), who inoculated mice with replicating MAIDS virus stocks containing various helper MuLVs. The only organ where the c-*myc* locus was found to be rearranged did not exhibit detectable clonal rearrangement of the J_H or C_κ region but showed a clonal TcRβ rearrangement, suggesting the expansion of a T-cell clone. In contrast, in the present study, the clonal population of cells infected by the MAIDS defective virus was of the B-cell lineage.

Since oligoclonal proliferation of the B cells infected by the MAIDS defective virus was found in all screened organs of diseased mice late after infection, and since the Dis-1–*Sfpi1* and Dis-2 loci were the targets of provirus insertion in only a small fraction of these organs, it is to be expected that some other loci contributing to this proliferation could be identified by the same strategy. As a precedent for this, van Lohuizen et al. (64) reported that four distinct loci were involved in cooperating with the Eμ-*myc* transgene independently, resulting in dramatic acceleration, through different pathways, of pre-B-cell lymphomagenesis in the animals.

The Spi-1/PU.1 locus is a target of provirus insertion in target cells infected with the MAIDS defective virus. Spi-1 was first identified as a common integration site in a very high percentage (95%) of spleen focus-forming virus-induced murine erythroleukemias (42). By sequence comparison, the product of the *Sfpi1* gene (Spi-1) was soon found to correspond to the PU.1 protein (19) and was identified independently as a transcription factor (32) and, more specifically, as a member of

the *Ets* oncogene family. In addition to erythroid cells, Spi-1 mRNA is normally present in B cells, in myelomonocytes, and in mast cells but not in T cells or nonhematopoietic cell types (17). The activity of this protein on transcription is regulated by phosphorylation (50). Spi-1 has been implicated in the regulation of expression of many genes, including those of the immunoglobulin heavy chain (53), λ chain (15), κ chain (50a), myeloid integrin (12), c-Fms (54), interleukin 3 (58), and the macrophage colony-stimulating factor (67) and glucocorticoid-inducible genes (18). It may also be involved in the regulation of the promoter of lentiviruses (8, 63). The putative oncogene identity of Spi-1 was strongly suggested by the rearrangement of this locus in 95% of the virus-induced erythroid tumors (42). In addition, Spi-1 has also been found to play a critical role in Rauscher MuLV-induced murine acute erythroleukemias (40). In long-term bone marrow cultures, PU.1 expression was shown to rapidly and efficiently immortalize erythroblasts (57), while chemicals which reduced PU.1 expression restored the erythropoietic differentiation program (56). In the present study, the MAIDS defective provirus was inserted within the Dis-1–*Sfpi1* locus of B cells, which have been found to constitute the majority of the infected cell population when helper-free stocks of the virus are used. To our knowledge, this is the first report of rearrangements of the *Sfpi1* (Spi-1/PU.1) locus detected in proliferating B cells.

The consequence of provirus integration within the Dis-1–*Sfpi1* locus appears to be modestly increased expression of this gene compared with the levels found in enlarged MAIDS lymphoid organs exhibiting no rearrangement. However, the level of Dis-1–*Sfpi1* expression in normal spleens is much lower, suggesting that uninfected cells or cells exhibiting no Dis-1 rearrangement present in MAIDS organs also exhibit higher levels of Dis-1–*Sfpi1* RNA. The small number of infected cells frequently detected in enlarged organs of MAIDS mice may mask higher levels of expression in these cells. Alternatively, modest enhancement of gene expression over that found in other proliferating cells may be sufficient to provide a selective growth advantage for cells harboring the integration close to Dis-1–*Sfpi1*.

Identification of a new locus, Dis-2, as a target for provirus integration in cells infected by the MAIDS defective virus. The Dis-2 locus maps on mouse chromosome 11, in the vicinity of *Erb-A*, *Erb-B2*, and *Csfg*, and appears to be a novel locus. Interestingly, the two proviruses inserted in the Dis-2 region were in opposite orientation. A similar pattern has been observed within the *Evi-3* region in some B-cell lymphomas (31). This contrasts with the usual pattern of integration of proviruses, in the same transcriptional orientation, seen around most genes targetted by MuLV proviruses, including the Dis-1–*Sfpi1* gene described here. Like the Dis-1–*Sfpi1* locus, the Dis-2 region is likely to harbor a gene involved in growth regulation, possibly specific to B cells. We looked in several tissues for the presence of Dis-2 specific RNA with a few of the unique-copy Dis-2 probes available, but this search was unsuccessful. Additional work is needed to identify the putative Dis-2-encoding gene dysregulated by the provirus integrations observed.

Development of MAIDS and clonal proliferation of infected B cells. The clonal or oligoclonal proliferation of B cells infected by the MAIDS defective virus is a relatively late event in the course of MAIDS and has been strongly correlated with the development of immune dysfunctions (28). Early after infection with the virus, this proliferation has been shown to be polyclonal (29). This polyclonal proliferation of infected B cells is also accompanied by early development of immune defects (59), suggesting that expansion of selected clones of infected B cells is not required for initiation of MAIDS and that all infected B cells contribute to this phenotype. The present study represents an important step toward the understanding of this polyclonal-to-oligoclonal transition by showing that the MAIDS defective virus can act as an insertional mutagen, activating a cellular oncogene(s), thus giving some infected cells an additional growth advantage. The provirus integrations in the vicinity of Dis-1–*Sfpi1*, Dis-2 or other, unknown loci are very likely to represent an early event, since nonreplicating helper-free stocks of the virus were used. Therefore, the growth advantage provided by these provirus integrations is likely to be modest, as they require a relatively long time (two to three months) before being detectable with the Southern technique used. An alternative possibility that may be less likely is that provirus insertions in Dis-1 or Dis-2 have no effect on cell growth by themselves and require the cooperation of other genes activated (or inactivated) later to promote mono- or oligoclonal cell growth. The modest effect of provirus insertions in Dis-1 and Dis-2, coupled with the fact that several common proviral integration sites appear to be targetted, suggests that the deregulation of each of these targetted loci is not essential for proliferation of infected B cells or development of immune dysregulation. This appears to contrast with the very frequent activation (95%) of one locus, Spi-1, by provirus in spleen focus-forming virus-induced erythroleukemia. Interestingly, our present data rule out a model of B-cell proliferation after infection with MAIDS defective viruses whereby only cells having sustained a specific integration event in the vicinity of a selected class of genes would acquire the ability to grow and to induce T-cell dysfunctions.

Therefore, the rapid proliferation of B cells infected by the MAIDS defective virus is most likely the consequence of early expression of the $Pr60^{gag}$ protein encoded by this virus and does not appear to be related primarily to a specific integration event of the defective provirus. The $Pr60^{gag}$ protein, in its myristylated form, has recently been shown to be required for development of MAIDS (24, 26, 51). It remains to be determined how the $Pr60^{gag}$ protein triggers the proliferation of its target B cells and how the proliferating, most likely reprogrammed, B cells induce a state of T-cell anergy. Our present results suggest that these events are not triggered by deregulation of a specific gene through provirus integration. However, it is very likely that the $Pr60^{gag}$ protein induces B cells to produce a factor(s) which directly or indirectly contributes to T-cell anergy.

ACKNOWLEDGMENTS

This work was supported by grants to Paul Jolicoeur from the Medical Research Council of Canada (MRC) and from the National Cancer Institute of Canada.

We are grateful to David Kabat and F. Moreau-Gachelin for providing Spi-1 cDNA. We thank Marie Bernier for typing the manuscript.

REFERENCES

1. **Adamson, M. C., J. Silver, and C. A. Kozak.** 1991. The mouse homolog of the Gibbon ape leukemia virus receptor: genetic mapping and a possible receptor function in rodents. Virology **183:**778–781.
2. **Aziz, D. C., Z. Hanna, and P. Jolicoeur.** 1989. Severe immunodeficiency disease induced by a defective murine leukaemia virus. Nature (London) **338:**505–508.
3. **Bargmann, C. I., M. C. Hung, and R. A. Weinberg.** 1986. Multiple independent activations of the neu oncogene by a point mutation altering the transmembrane domain of p185. Cell **45:**649–657.
4. **Bentley, K. L., M. S. Bradshaw, and F. H. Ruddle.** 1993. Physical linkage of the murine Hox-b cluster and nerve growth factor receptor on yeast artificial chromosomes. Genomics **18:**43–53.
5. **Berger, M. S., C. A. Kozak, A. Gabriel, and M. B. Prystowsky.** 1993. The gene for C10, a member of the beta-chemokine family, is located on mouse

chromosome 11 and contains a novel second exon not found in other chemokines. DNA Cell Biol. **12:**839–847.
6. **Buchberg, A. M., H. G. Bedigian, N. A. Jenkins, and N. G. Copeland.** 1990. *Evi-2*, a common integration site involved in murine myeloid leukemogenesis. Mol. Cell. Biol. **10:**4658–4666.
7. **Buchberg, A. M., and S. A. Camper.** 1993. Encyclopedia of the mouse genome III. October 1993. Mouse chromosome 11. Mamm. Genome **4:**S164–S175.
8. **Carvalho, M., and D. Derse.** 1993. The PU.1/Spi-1 proto-oncogene is a transcriptional regulator of a lentivirus promoter. J. Virol. **67:**3885–3890.
9. **Chakraborti, A., and C. A. Kozak.** 1992. Microtubule-associated genes (Mtap-1, Mtap-2, Mtap-5) map to mouse chromosomes 1, 2, and 13. Mouse Genome **90:**679–681.
10. **Chattopadhyay, S. K., H. C. Morse III, M. Makino, S. K. Ruscetti, and J. W. Hartley.** 1989. Defective virus is associated with induction of murine retrovirus-induced immunodeficiency syndrome. Proc. Natl. Acad. Sci. USA **86:** 3862–3866.
11. **Chattopadhyay, S. K., D. N. Sengupta, T. N. Fredrickson, H. C. Morse III, and J. W. Hartley.** 1991. Characteristics and contributions of defective, ecotropic, and mink cell focus-inducing viruses involved in a retrovirus-induced immunodeficiency syndrome of mice. J. Virol. **65:**4232–4241.
12. **Chen, H. M., H. L. Pahl, R. J. Scheibe, D. E. Zhang, and D. G. Tenen.** 1993. The Sp1 transcription factor binds the CD11b promoter specifically in myeloid cells in vivo and is essential for myeloid-specific promoter activity. J. Biol. Chem. **268:**8230–8239.
13. **Chomczynski, P., and N. Sacchi.** 1987. Single-step method of RNA isolation by acid guanidinium thiocyanate-phenol-chloroform extraction. Anal. Biochem. **162:**156–159.
14. **Cuypers, H. T., G. Selten, W. Quint, M. Zijlstra, E. R. Maandag, W. Boelens, P. van Wezenbeek, C. Melief, and A. Berns.** 1984. Murine leukemia virus-induced T-cell lymphomagenesis: integration of proviruses in a distinct chromosomal region. Cell **37:**141–150.
15. **Eisenbeis, C. F., H. Singh, and U. Storb.** 1993. PU.1 is a component of a multiprotein complex which binds an essential site in the murine immunoglobulin λ2-4 enhancer. Mol. Cell. Biol. **13:**6452–6461.
16. **Feinberg, A. P., and B. Vogelstein.** 1983. A technique for radiolabeling DNA restriction endonuclease fragments to high specific activity. Anal. Biochem. **132:**6–13.
17. **Galson, D. L., J. O. Hensold, T. R. Bishop, M. Schalling, A. D. D'Andrea, C. Jones, P. E. Auron, and D. E. Housman.** 1993. Mouse β-globin DNA-binding protein B1 is identical to a proto-oncogene, the transcription factor *Spi-1*/PU.1, and is restricted in expression to hematopoietic cells and the testis. Mol. Cell. Biol. **13:**2929–2941.
18. **Gauthier, J. M., B. Bourachot, V. Doucas, M. Yaniv, and F. Moreau-Gachelin.** 1993. Functional interference between the Spi-1/PU.1 oncoprotein and steroid hormone or vitamin receptors. EMBO J. **12:**5089–5096.
19. **Goebl, M. G.** 1990. The PU.1 transcription factor is the product of the putative oncogene Spi-1. Cell **61:**1165–1166.
20. **Goff, S. P.** 1992. Genetics of retroviral integration. Annu. Rev. Genet. **26:** 527–544.
21. **Gonda, T. J., N. M. Gough, A. R. Dunn, and J. de Blaquière.** 1985. Nucleotide sequence of cDNA clones of the murine myb proto-oncogene. EMBO J. **4:**2003–2008.
22. **Green, E. L.** 1981. Genetics and probability in animal breeding experiments, p. 79–113. Oxford University Press, New York.
23. **Hake, L. E., N. Kuemmerle, N. B. Hecht, and C. A. Kozak.** 1994. The genes encoding the somatic and testis-specific isotypes of the mouse cytochrome c genes map to paralogous regions of chromosomes 6 and 2. Genomics **20:** 503–505.
24. **Huang, M., Z. Hanna, and P. Jolicoeur.** 1995. Mutational analysis of the murine AIDS-defective viral genome reveals a high reversion rate in vivo and a requirement for an intact $Pr60^{gag}$ protein for efficient induction of disease. J. Virol. **69:**60–68.
25. **Huang, M., and P. Jolicoeur.** 1990. Characterization of the *gag*/fusion protein encoded by the defective Duplan retrovirus inducing murine acquired immunodeficiency syndrome. J. Virol. **64:**5764–5772.
26. **Huang, M., and P. Jolicoeur.** 1994. Myristylation of $Pr60^{gag}$ of the murine AIDS-defective virus is required to induce disease and notably for the expansion of its target cells. J. Virol. **68:**5648–5655.
27. **Huang, M., C. Simard, and P. Jolicoeur.** 1989. Immunodeficiency and clonal growth of target cells induced by helper-free defective retrovirus. Science **246:**1614–1617.
28. **Huang, M., C. Simard, and P. Jolicoeur.** 1992. Susceptibility of inbred strains of mice to murine AIDS (MAIDS) correlates with target cell expansion and high expression of defective MAIDS virus. J. Virol. **66:**2398–2406.
29. **Huang, M., C. Simard, D. G. Kay, and P. Jolicoeur.** 1991. The majority of cells infected with the defective murine AIDS virus belong to the B-cell lineage. J. Virol. **65:**6562–6571.
30. **Jolicoeur, P.** 1991. The murine acquired immunodeficiency syndrome (MAIDS): an animal model to study the AIDS pathogenesis. FASEB J. **5:**2398–2405.
31. **Justice, M. J., H. C. Morse III, N. A. Jenkins, and N. G. Copeland.** 1994. Identification of *Evi-3*, a novel common site of retroviral integration in mouse AKXD B-cell lymphomas. J. Virol. **68:**1293–1300.
32. **Klemsz, M. J., S. R. McKercher, A. Celada, C. Van Beveren, and R. A. Maki.** 1990. The macrophage and B cell-specific transcription factor PU.1 is related to the ets oncogene. Cell **61:**113–124.
33. **Klinken, S. P., T. N. Fredrickson, J. W. Hartley, R. A. Yetter, and H. C. Morse III.** 1988. Evolution of B cell lineage lymphomas in mice with a retrovirus-induced immunodeficiency syndrome, MAIDS. J. Immunol. **140:** 1123–1131.
34. **Kozak, C. A., M. Danciger, C. Bowes, M. C. Adamson, K. Palczewski, A. S. Polans, and D. B. Farber.** 1995. Localization of three genes expressed in retina on mouse chromosome 11. Mamm. Genome **6:**142–144.
35. **Kozak, C. A., M. Peyser, M. Krall, T. M. Mariano, C. S. Kumar, S. Pestka, and B. A. Mock.** 1990. Molecular genetic markers spanning mouse chromosome 10. Genomics **8:**519–524.
36. **Kung, H. J., C. Boerkoel, and T. H. Carter.** 1991. Retroviral mutagenesis of cellular oncogenes: a review with insights into the mechanisms of insertion activation. Curr. Top. Microbiol. Immunol. **171:**1–25.
37. **Land, H., L. F. Parada, and R. A. Weinberg.** 1983. Tumorigenic conversion of primary embryo fibroblasts requires at least two cooperating oncogenes. Nature (London) **304:**596–602.
38. **Lemay, G., and P. Jolicoeur.** 1984. Rearrangement of a DNA sequence homologous to a cell-virus junction fragment in several Moloney murine leukemia virus-induced rat thymomas. Proc. Natl. Acad. Sci. USA **81:**38–42.
39. **Maniatis, T., E. F. Fritsch, and J. Sambrook.** 1982. Molecular cloning: a laboratory manual, 2nd ed. Cold Spring Harbor Laboratory Press, Cold Spring Harbor, N.Y.
40. **Moreau-Gachelin, F., D. Ray, N. J. de Both, M. J. van der Feltz, P. Tambourin, and A. Tavitian.** 1990. Spi-1 oncogene activation in Rauscher and Friend murine virus-induced acute erythroleukemias. Leukemia **4:**20–23.
41. **Moreau-Gachelin, F., D. Ray, M. G. Mattei, P. Tambourin, and A. Tavitian.** 1989. The putative oncogene Spi-1: murine chromosomal localization and transcriptional activation in murine acute erythroleukemias. Oncogene **4:**1449–1456.
42. **Moreau-Gachelin, F., A. Tavitian, and P. Tambourin.** 1988. Spi-1 is a putative oncogene in virally induced murine erythroleukaemias. Nature (London) **331:**277–280.
43. **Morse, H. C., III, S. K. Chattopadhyay, M. Makino, T. N. Fredrickson, A. W. Hugin, and J. W. Hartley.** 1992. Retrovirus-induced immunodeficiency in the mouse: MAIDS as a model for AIDS. AIDS **6:**607–621.
44. **Mosier, D. E.** 1986. Animal models for retrovirus-induced immunodeficiency disease. Immunol. Invest. **15:**233–261.
45. **Paul, R., S. Schuetze, S. L. Kozak, and D. Kabat.** 1989. A common site for immortalizing proviral integrations in Friend erythroleukemia: molecular cloning and characterization. J. Virol. **63:**4958–4961.
46. **Peters, G.** 1990. Oncogenes at viral integration sites. Cell Growth Differ. **1:**503–510.
47. **Pilon, A. L., C. A. Kozak, D. W. Nebert, and A. Puga.** 1993. Localization of the murine Hmg1 gene, encoding an HMG-box protein, to mouse chromosome 2. Mamm. Genome **4:**612–614.
48. **Poirier, Y., and P. Jolicoeur.** 1989. Distinct helper virus requirements for Abelson murine leukemia virus-induced pre-B- and T-cell lymphomas. J. Virol. **63:**2088–2098.
49. **Poirier, Y., C. Kozak, and P. Jolicoeur.** 1988. Identification of a common helper provirus integration site in Abelson murine leukemia virus-induced lymphoma DNA. J. Virol. **62:**3985–3992.
50. **Pongubala, J. M., C. Van Beveren, S. Nagulapalli, M. J. Klemsz, S. R. McKercher, R. A. Maki, and M. L. Atchison.** 1993. Effect of PU.1 phosphorylation on interaction with NF-EM5 and transcriptional activation. Science **259:**1622–1625.
50a. **Pongubala, J. M. R., S. Nagulapalli, M. J. Klemsz, S. R. McKercher, R. A. Maki, and M. L. Atchinson.** 1992. PU.1 recruits a second nuclear factor to a site important for immunoglobulin κ 3′ enhancer activity. Mol. Cell. Biol. **12:**368–378.
51. **Pozsgay, J. M., M. W. Beilharz, B. D. Wines, A. D. Hess, and P. M. Pitha.** 1993. The MA (p15) and p12 regions of the *gag* gene are sufficient for the pathogenicity of the murine AIDS virus. J. Virol. **67:**5989–5999.
52. **Pryciak, P. M., and H. E. Varmus.** 1992. Nucleosomes, DNA-binding proteins, and DNA sequence modulate retroviral integration target site selection. Cell **69:**769–780.
53. **Rivera, R., M. H. Stuiver, R. Steenbergen, and C. Murre.** 1993. Ets proteins: new factors that regulate immunoglobulin heavy-chain gene expression. Mol. Cell. Biol. **13:**7163–7169.
54. **Ross, I. L., T. L. Dunn, X. Yue, S. Roy, C. J. Barnett, and D. A. Hume.** 1994. Comparison of the expression and function of the transcription factor PU.1 (Spi-1 proto-oncogene) between murine macrophages and B lymphocytes. Oncogene **9:**121–132.
55. **Savard, P., L. DesGroseillers, E. Rassart, Y. Poirier, and P. Jolicoeur.** 1987. Important role of the long terminal repeat of the helper Moloney murine leukemia virus in Abelson virus-induced lymphoma. J. Virol. **61:**3266–3275.
56. **Schuetze, S., R. Paul, B. C. Gliniak, and D. Kabat.** 1992. Role of the PU.1 transcription factor in controlling differentiation of Friend erythroleukemia

cells. Mol. Cell. Biol. **12:**2967–2975.
57. **Schuetze, S., P. E. Stenberg, and D. Kabat.** 1993. The Ets-related transcription factor PU.1 immortalizes erythroblasts. Mol. Cell. Biol. **13:**5670–5678.
58. **Shimada, Y., G. Migliaccio, S. Ruscetti, J. W. Adamson, and A. R. Migliaccio.** 1992. Expression of the interleukin-3 and granulocyte-macrophage colony-stimulating factor genes in Friend spleen focus-forming virus-induced erythroleukemia. Blood **79:**2423–2431.
59. **Simard, C., M. Huang, and P. Jolicoeur.** 1994. Murine AIDS is initiated in the lymph nodes draining the site of inoculation, and the infected B cells influence T cells located at distance, in noninfected organs. J. Virol. **68:**1903–1912.
60. **Simek, S. L., C. A. Kozak, D. Winterstein, G. Hegamyer, and N. H. Colburn.** 1993. Sequence and localization of a novel FK506-binding protein to mouse chromosome 11. Genomics **18:**407–409.
61. **Southern, E. M.** 1975. Detection of sequences among DNA fragments separated by gel electrophoresis. J. Mol. Biol. **38:**503–517.
62. **Tremblay, P. J., C. A. Kozak, and P. Jolicoeur.** 1992. Identification of a novel gene, *Vin-1*, in murine leukemia virus-induced T-cell leukemias by provirus insertional mutagenesis. J. Virol. **66:**1344–1353.
63. **Van Lint, C., J. Ghysdael, P. J. Paras, A. Burny, and E. Verdin.** 1994. A transcriptional regulatory element is associated with a nuclease-hypersensitive site in the *pol* gene of human immunodeficiency virus type 1. J. Virol. **68:**2632–2648.
64. **van Lohuizen, M., S. Verbeek, B. Scheijen, E. Wientjens, H. van der Gulden, and A. Berns.** 1991. Identification of cooperating oncogenes in E mu-myc transgenic mice by provirus tagging. Cell **65:**737–752.
65. **Vennstrom, B., and J. M. Bishop.** 1982. Isolation and characterization of chicken DNA homologous to the two putative oncogenes of avian erythroblastosis virus. Cell **28:**135–143.
66. **Villemur, R., Y. Monczak, E. Rassart, C. Kozak, and P. Jolicoeur.** 1987. Identification of a new common provirus integration site in Gross passage A murine leukemia virus-induced mouse thymoma DNA. Mol. Cell. Biol. **7:**512–522.
67. **Zhang, D.-E., C. J. Hetherington, H.-M. Chen, and D. G. Tenen.** 1994. The macrophage transcription factor PU.1 directs tissue-specific expression of the macrophage colony-stimulating factor receptor. Mol. Cell. Biol. **14:**373–381.